Liu *et al. EURASIP Journal on Wireless Communications and Networking* (2016) 2016:135
DOI 10.1186/s13638-016-0615-3

EURASIP Journal on Wireless Communications and Networking

RESEARCH Open Access

SER analysis of the MRC-OFDM receiver with pulse blanking over frequency selective fading channel

Haitao Liu[1*†], Zhisheng Yin[2†], Min Jia[2] and Xuejun Zhang[3]

Abstract

Pulse blanking is a widely used method to eliminate impulsive interference in an orthogonal frequency division multiplexing (OFDM) receiver. To analyze the effect of the inter-carrier interference caused by pulse blanking on the symbol error rate (SER) performance of OFDM employing maximum ratio combining (MRC) receiver, the analytical expression of the signal-to-interference-noise ratio (SINR) of the OFDM employing MRC receiver is derived. Based on the SINR expression, furthermore, the SER performances over both Rayleigh and Ricean fading channels are also analyzed quantitatively. Simulation results validate the correctness of the derived formulas.

Keywords: OFDM, MRC, Impulse interference, Pulse blanking, SINR, SER, Rayleigh, Ricean

1 Introduction

Orthogonal frequency division multiplexing (OFDM) is a multicarrier modulation technique which converts a frequency-selective channel into a parallel collection of frequency flat subchannels. Compared with single-carrier communication systems, OFDM has advantages, such as spectral efficiency, efficient implementation based on the fast Fourier transform (FFT), and simple channel equalization. For these reasons, the OFDM transmission scheme is widely employed in wireless and wired communications, e.g., digital subscriber lines (DSL), digital video broadcasting (DVB), digital audio broadcasting (DAB), wireless local area networks (WLAN), power line communications (PLC), long term evolution (LTE), and L-band digital aeronautical communication system (L-DACS) [1].

In practical applications, OFDM systems are often exposed to impulsive interference, e.g., ignition noise of passing vehicles, impulsive noise in power line or other systems operating in the same frequency range. Some studies have shown that the impulse interference with high power or frequent occurrence can significantly affect the performance of OFDM receivers [2, 3]. Thus, it is of great significance to eliminate the impulse interference in OFDM receivers.

To suppress the effect of impulsive noise on an OFDM receiver, an interference mitigation method based on pulse blanking is first proposed in [4–6]. However, when using this method to an actual system, two problems should be considered, the threshold of pulse blanking and the compensation of inter-carrier interference (ICI) caused by pulse blanking. To calculate the blanking threshold, an optimal threshold of pulse blanking is derived based on an expression for the signal-to-noise ratio (SNR) of the blanking nonlinearity [7]. With maximizing the signal-to-interference-and-noise ratio (SINR) criterion, an adaptive blanking threshold for the OFDM receiver is also proposed in [8]. To eliminate the ICI caused by pulse blanking, an iterative reconstructing and subtracting ICI method is proposed in [9, 10], and a frequency-domain ICI compensation scheme based on finite impulse response equalizer is proposed in [11].

Studies on the performance analysis of single-carrier systems in impulsive noise environment are presented in [12–16]. The performance of diversity combining technique over fading channels with impulsive noise is analyzed in [12]. Adopting the Middleton class A impulsive noise model, the performance of space-time coded systems over multiple-input multiple-output (MIMO) channels with impulsive noise is studied in [13, 14]. The effect

*Correspondence: htliucauc@qq.com
†Equal contributors
[1]Tianjin Key Lab for Advanced Signal Processing, Civil Aviation University of China, 30030 Tianjin, China
Full list of author information is available at the end of the article

of symmetric α-stable noise on space-time coded systems over MIMO fading channels is analyzed in [15]. A unified mathematical framework for the analysis of the asymptotic performance of amplify-and-forward cooperative diversity systems impaired by generic noise is provided in [16]. The influence of impulse noise on the symbol error rate (SER) performances of multicarrier and single-carrier communication systems is investigated and compared in [2]. With regard to the performance analysis of the OFDM receiver with blanking, the SNR expression of the OFDM receiver with blanking is obtained for the AWGN channel [17]. The SNR expression for the OFDM receiver with blanking is derived in frequency selective Rayleigh fading channel, as well as the SER performance on this SNR expression [18]. To the best of our knowledge, there is currently no literature regarding the SER performance of the maximum ratio combining (MRC)-OFDM receiver with pulse blanking.

In this paper, a closed-form expression for the SINR of the MRC-OFDM receiver with pulse blanking over frequency selective fading channel is derived. Furthermore, the SER performances of the MRC-OFDM receiver with pulse blanking over both Rayleigh and Ricean fading channels are also analyzed quantitatively based on this SINR expression. Finally, simulation results are presented that validate the correctness of the derived formulas.

This paper is arranged as follows. In Section 2, a system model comprising the OFDM transmitter and the MRC-OFDM receiver with pulse blanking is introduced. In Section 3, the closed-from expression for the SINR of the MRC-OFDM receiver with pulse blanking is derived, and the SER performances for both Rayleigh and Ricean fading channels are also analyzed. In Section 4, an overview of system and channel parameters is provided, and the analytically calculated and simulated symbol error performance curves are presented to validate our theoretical results. In Section 5, we draw the main conclusion.

2 System model

2.1 OFDM transmitter

The model for the OFDM transmitter is shown in Fig. 1. An information bit sequence is sent to the modulator for symbol mapping. The output symbol vector of the modulator is denoted as $\mathbf{S} = [S_0, \ldots, S_k, \ldots, S_{K-1}]^T$, where K denotes the number of complex modulated symbols, and $\{S_k, k = 0, 1, \ldots, K-1\}$ are assumed to be independent and identically distributed (i.i.d.) with $E\{S_k\} = 0$ and $E\left\{|S_k|^2\right\} = \sigma_S^2$.

The modulated symbol vector $\mathbf{S}$ is then transformed into the time domain by the K-point inverse fast Fourier transform (IFFT), and the output signal vector of IFFT is given by

$$\mathbf{s} = \mathbf{F}^H \mathbf{S} \tag{1}$$

where IFFT matrix $\mathbf{F}^H$ is defined by

$$\mathbf{F}_{n,k}^H = \frac{1}{\sqrt{K}} e^{2\pi j \frac{kn}{K}}, \quad n, k = 0, 1, \cdots, K-1 \tag{2}$$

with k being the subcarrier index in the frequency domain and n denoting the sample index in the time domain. As IFFT is a unitary transformation, the statistical property of $\mathbf{s}$ agrees with $\mathbf{S}$, and $\{s_n, n = 0, 1, \ldots, K-1\}$ are also i.i.d. with $E\{s_n\} = 0$ and $E\left\{|s_n|^2\right\} = \sigma_S^2$.

After inserting the K_g-point cyclic prefix, the transmitted signal vector $\mathbf{x} = \left[x_0, \ldots, x_n, \ldots, x_{K+K_g-1}\right]^T$ can be expressed as

$$\mathbf{x} = \mathbf{P}_{\text{in}} \mathbf{s} \tag{3}$$

where $\mathbf{P}_{\text{in}}$ is the cyclic prefix insertion matrix denoted as

$$\mathbf{P}_{\text{in}} = \begin{bmatrix} \mathbf{0}_{K_g \times (K-K_g)} & \mathbf{I}_{K_g} \\ & \mathbf{I}_K \end{bmatrix}_{(K+K_g)\times K} \tag{4}$$

where $\mathbf{0}_{K\times(K-K_g)}$ is a $K_g \times (K - K_g)$ zero matrix and $\mathbf{I}_K$ is a $K \times K$ identity matrix.

The transmitted signal vector $\mathbf{x}$ is then converted to an analog signal $x(t)$ by the D/A converter and $x(t)$ is transformed into a RF signal by the RF front end. Finally, the RF signal is sent to a channel by the transmitter antenna.

2.2 MRC-OFDM receiver with pulse blanking

The model for the MRC-OFDM receiver with pulse blanking is depicted in Fig. 2. The received baseband signal from the vth antenna can be represented as

$$r^v(t) = x(t) * h^v(t) + n^v(t) + i^v(t), v = 1, 2, \ldots, N \tag{5}$$

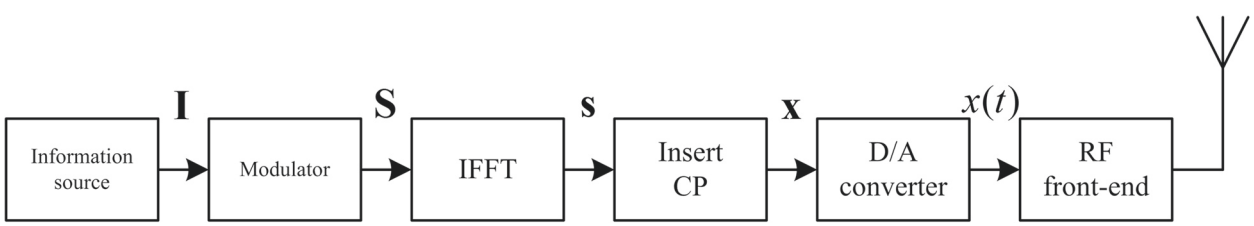

Fig. 1 Block diagram of the OFDM transmitter

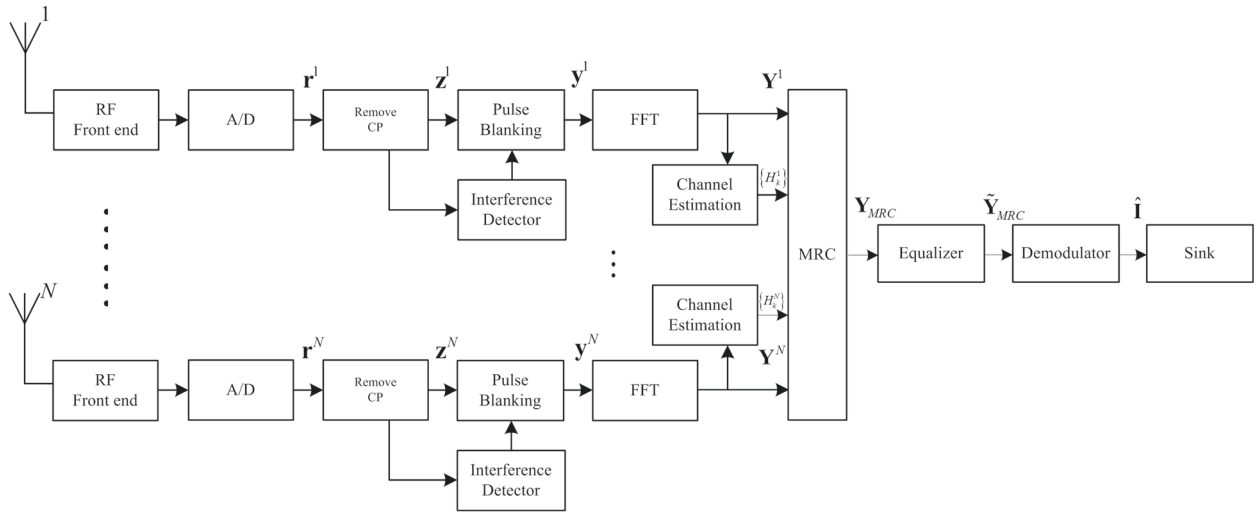

Fig. 2 Block diagram of the MRC-OFDM receiver with pulse blanking

where $x(t)$ denotes the transmitted signal, $*$ the convolution operation, $h^{\nu}(t)$ the channel impulse response of the νth channel, $n^{\nu}(t)$ the complex Gaussian white noise signal from the νth channel, $i^{\nu}(t)$ the impulsive noise from the νth channel, and N the number of receive antenna.

Assuming that the symbol timing synchronization has been established, the transmitted signal $r^{\nu}(t)$ is then converted to a sampled signal vector $\mathbf{r}^{\nu}$ by the A/D converter. After removing the K_g-point cyclic prefix, the received signal vector can be expressed as

$$\mathbf{z}^{\nu} = \mathbf{P}_{\text{out}}\mathbf{r}^{\nu}, \nu = 1, 2, \ldots, N \tag{6}$$

where $\mathbf{P}_{\text{out}} = \left[\mathbf{0}_{K\times K_g} \quad \mathbf{I}_K\right]$ denotes the cyclic prefix removal matrix.

According to the basic theory of OFDM [19], $\mathbf{z}^{\nu}$ can be written as

$$\mathbf{z}^{\nu} = \mathbf{s} \otimes \mathbf{h}^{\nu} + \mathbf{i}^{\nu} + \mathbf{n}^{\nu}, \nu = 1, 2 \ldots, N \tag{7}$$

where $\mathbf{s}$ is given by Eq. (1), $\otimes$ denotes the circular convolution operator, and $\mathbf{h}^{\nu} = \left[h_0^{\nu}, \ldots, h_l^{\nu}, \ldots, h_{L_{\nu}-1}^{\nu}\right]^T$ is the discrete-time channel impulse response of the νth channel with L_{ν} paths, where $\left\{h_l^{\nu}, l = 0, 1 \ldots, L_{\nu} - 1\right\}$ are assumed to be i.i.d. and remain constant over one OFDM symbol interval, and the channel power is normalized to 1, i.e., $\sum_{l=0}^{L-1} E\left\{\left|h_l^{\nu}\right|^2\right\} = 1$. In addition, $\mathbf{n}^{\nu} = \left[n_0^{\nu}, \ldots, n_n^{\nu}, \ldots, n_{K-1}^{\nu}\right]^T$ denotes the complex Gaussian white noise vector from the νth channel where $\left\{n_n^{\nu}, n = 0, 1, \ldots, K-1\right\}$ are the i.i.d. complex Gaussian random variables (RVs) of mean zeros and variance δ_n^2 and $\mathbf{i}^{\nu} = \left[i_0^{\nu}, \ldots, i_n^{\nu}, \ldots, i_{K-1}^{\nu}\right]^T$ denotes the impulsive noise vector where i_n^{ν} is modeled as a Bernoulli-Gaussian RV [2]

$$i_n^{\nu} = b_n^{\nu} g_n^{\nu}, n = 0, 1, \ldots, K-1, \nu = 1, 2, \ldots, N \tag{8}$$

where b_n^{ν} is the Bernoulli process which is the arrival of impulsive noise with probability $\mathrm{P_r}\left(b_n^{\nu} = 1\right) = p$ and g_n^{ν} is the complex Gaussian RV with mean zeros and variance $\delta_g^{\nu 2}$.

Assuming that the positions of the impulsive noise occurrence are precisely detected by the interference detector, the output of the impulse blanking $\mathbf{y}^{\nu} = \left[y_0^{\nu}, \ldots, y_n^{\nu}, \ldots, y_{K-1}^{\nu}\right]^T$ is given as

$$\mathbf{y}^{\nu} = \bar{\mathbf{B}}^{\nu}\mathbf{z}^{\nu}, \nu = 1, 2, \ldots, N \tag{9}$$

where $\bar{\mathbf{B}}^{\nu}$ denotes the impulse blanking matrix for the νth receive branch and where $\bar{\mathbf{B}}^{\nu} = \mathrm{diag}\left(\bar{b}_0^{\nu}, \ldots, \bar{b}_n^{\nu}, \ldots, \bar{b}_{K-1}^{\nu}\right)$ with $\bar{b}_n^{\nu} = 1 - b_n^{\nu}$.

The signal vector $\mathbf{y}^{\nu}$ is then transformed into the frequency domain by the K-point fast Fourier transform (FFT). Hence, the output signal vector of FFT $\mathbf{Y}^{\nu} = \left[Y_0^{\nu}, \ldots, Y_k^{\nu}, \ldots, Y_{K-1}^{\nu}\right]^T$ is given by

$$\mathbf{Y}^{\nu} = \mathbf{F}\mathbf{y}^{\nu}, \nu = 1, 2, \ldots, N \tag{10}$$

where the FFT matrix $\mathbf{F}$ is defined by

$$\mathbf{F}_{k,n} = \frac{1}{\sqrt{K}} e^{-2\pi j \frac{kn}{K}}, \quad k, n = 0, 1, \ldots, K-1 \tag{11}$$

Assuming that the ideal channel estimation is employed, the output signal vector of the maximum ratio combiner is given as

$$\mathbf{Y}_{\text{MRC}} = \sum_{\nu=1}^{N} \left(\mathbf{H}^{\nu}\right)^* \mathbf{Y}^{\nu} \tag{12}$$

where $\mathbf{H}^{\nu} = \mathrm{diag}\left(H_0^{\nu}, .., H_k^{\nu}, \ldots, H_{K-1}^{\nu}\right)$ denotes the frequency domain channel transfer matrix of the νth channel and H_k^{ν} denotes the frequency response of the kth subchannel for the νth channel.

We assume that a linear forced zero equalizer is employed in the receiver. The output of the equalizer is given as $\tilde{\mathbf{Y}}_{\mathrm{MRC}} = \left[\tilde{Y}_{\mathrm{MRC},0}, \ldots, \tilde{Y}_{\mathrm{MRC},k}, \ldots, \tilde{Y}_{\mathrm{MRC},K-1}\right]^T$, where $\tilde{Y}_{\mathrm{MRC},k}$ denotes the output signal of the equalizer for the kth subchannel, which is given by

$$\tilde{Y}_{\mathrm{MRC},k} = \frac{\sum_{\nu=1}^{N} \left(H_k^{\nu}\right)^* Y_k^{\nu}}{\sum_{\nu=1}^{N} \left|H_k^{\nu}\right|^2}, k = 0, 1 \ldots, K-1 \tag{13}$$

The signal vector $\tilde{\mathbf{Y}}_{\mathrm{MRC}}$ is finally sent to the demodulator, where the output bit sequence $\hat{\mathbf{I}}$ is sent to the sink.

3 Performance analysis

3.1 SINR for the MRC-OFDM demodulator

Substituting Eq. (7) into Eq. (9), the output signal vector of the pulse blanking can be represented as

$$\mathbf{y}^{\nu} = \bar{\mathbf{B}}^{\nu}(\mathbf{s} \otimes \mathbf{h}^{\nu}) + \bar{\mathbf{B}}^{\nu}\mathbf{i}^{\nu} + \bar{\mathbf{B}}^{\nu}\mathbf{n}^{\nu}, \nu = 1, 2, \ldots, N \tag{14}$$

where $\bar{\mathbf{B}}^{\nu}\mathbf{i}^{\nu} = \mathrm{diag}\left(\bar{b}_0^{\nu} i_0^{\nu}, \ldots, \bar{b}_n^{\nu} i_n^{\nu}, \ldots, \bar{b}_{K-1}^{\nu} i_{K-1}^{\nu}\right)$ with the nth component represented as

$$\begin{aligned} \bar{b}_n^{\nu} i_n^{\nu} = \left(1 - b_n^{\nu}\right) b_n^{\nu} g_n^{\nu}, \quad & n = 0, 1, \ldots, K-1, \\ & \nu = 1, 2, \ldots, N \end{aligned} \tag{15}$$

As b_n^{ν} is a Bernoulli RV that takes a value of one or zero, the product $(1 - b_n)\, b_n$ identically equals to 0, thus $\bar{b}_n^{\nu} i_n^{\nu} = 0$, and then $\bar{\mathbf{B}}\mathbf{i} = \mathbf{0}$. Given all the above, Eq. (14) is further simplified as

$$\mathbf{y}^{\nu} = \mathbf{s} \otimes \mathbf{h}^{\nu} + \tilde{\mathbf{i}}^{\nu} + \tilde{\mathbf{n}}^{\nu}, \nu = 1, 2 \ldots, N \tag{16}$$

where $\tilde{\mathbf{i}}^{\nu} = \left(\bar{\mathbf{B}}^{\nu} - \mathbf{I}\right)(\mathbf{s} \otimes \mathbf{h}^{\nu})$ denotes the equivalent impulse noise vector with the nth component represented as

$$\tilde{i}_n^{\nu} = -b_n^{\nu} \sum_{m=0}^{K-1} s_m h_{(n-m) \bmod K}^{\nu}, \nu = 1, 2, \ldots, \tag{17}$$

and $\tilde{\mathbf{n}}^{\nu} = \bar{\mathbf{B}}^{\nu}\mathbf{n}^{\nu}$ denotes the complex Gaussian white noise vector in the output of pulse blanking with the nth component $\tilde{n}_n^{\nu}$ represented as

$$\tilde{n}_n^{\nu} = \left(1 - b_n^{\nu}\right) n_n^{\nu}, \nu = 1, 2, \ldots, N \tag{18}$$

Substituting Eq. (16) into Eq. (10) yields

$$\mathbf{Y}^{\nu} = \mathbf{S}\mathbf{H}^{\nu} + \mathbf{F}\tilde{\mathbf{i}}^{\nu} + \mathbf{F}\tilde{\mathbf{n}}^{\nu}, \nu = 1, 2, \ldots, N \tag{19}$$

Expanding Eq. (19), the kth component of $\mathbf{Y}^{\nu}$ can be expressed as

$$\begin{aligned} Y_k^{\nu} = S_k H_k^{\nu} &+ \frac{1}{\sqrt{K}} \sum_{n=0}^{K-1} \tilde{i}_n^{\nu} e^{-2\pi j \frac{kn}{K}} \\ &+ \frac{1}{\sqrt{K}} \sum_{n=0}^{K-1} \tilde{n}_n^{\nu} e^{-2\pi j \frac{k \cdot n}{K}} \end{aligned} \tag{20}$$

Substituting Eq. (20) into Eq. (13), the kth component of $\mathbf{Y}_{\mathrm{MRC}}$ can be expressed as

$$\begin{aligned} Y_{\mathrm{MRC},k} =& S_k \sum_{\nu=1}^{N} \left|H_k^{\nu}\right|^2 \\ &+ \frac{1}{\sqrt{K}} \sum_{\nu=1}^{N} \left(H_k^{\nu}\right)^* \sum_{n=0}^{K-1} \tilde{i}_n^{\nu} e^{-2\pi j \frac{kn}{K}} \\ &+ \frac{1}{\sqrt{K}} \sum_{\nu=1}^{N} \left(H_k^{\nu}\right)^* \sum_{n=0}^{K-1} \tilde{n}_n^{\nu} e^{-2\pi j \frac{kn}{K}} \end{aligned} \tag{21}$$

From Eq. (21), $Y_{\mathrm{MRC},k}$ can be split into two parts, the first containing the desired signal of the kth subchannel, denoted by E_k, and the second containing the noise and the ICI caused by pulse blanking, denoted by W_k. $Y_{\mathrm{MRC},k}$ can be further expressed as

$$Y_{\mathrm{MRC},k} = E_k + W_k \tag{22}$$

where

$$E_k = S_k \sum_{\nu=1}^{N} \left|H_k^{\nu}\right|^2 \tag{23}$$

and

$$\begin{aligned} W_k =& \frac{1}{\sqrt{K}} \sum_{\nu=1}^{N} \left(H_k^{\nu}\right)^* \sum_{n=0}^{K-1} \tilde{i}_n^{\nu} e^{-2\pi j \frac{kn}{K}} \\ &+ \frac{1}{\sqrt{K}} \sum_{\nu=1}^{N} \left(H_k^{\nu}\right)^* \sum_{n=0}^{K-1} \tilde{n}_n^{\nu} e^{-2\pi j \frac{kn}{K}} \end{aligned} \tag{24}$$

The variance of E_k is given as

$$V_{\mathrm{ar}}\left(E_k\right) = \sigma_S^2 \left(\sum_{\nu=1}^{N} \left|H_k^{\nu}\right|^2\right)^2 \tag{25}$$

From the derivation in the Appendix, the variance of W_k can be calculated as

$$V_{\mathrm{ar}}\left(W_k\right) = \left[p\sigma_S^2 + (1-p)\,\delta_n^2\right] \sum_{\nu=1}^{N} \left|H_k^{\nu}\right|^2 \tag{26}$$

Combining Eqs. (25) and (26), the instantaneous SINR of the kth subchannel at the output of MRC is given as

$$\gamma_k \triangleq \frac{V_{\text{ar}}(E_k)}{V_{\text{ar}}(W_k)} = \sum_{\nu=1}^{N} \frac{\sigma_S^2}{p\sigma_S^2 + (1-p)\delta_n^2} \left|H_k^\nu\right|^2, \quad k = 0, 1, \ldots, K-1 \tag{27}$$

Let $\rho \triangleq \delta_S^2 / \delta_n^2$ denote the average input SNR per antenna (channel), Eq. (27) becomes

$$\gamma_k = \sum_{\nu=1}^{N} \frac{\rho}{p\rho + (1-p)} \left|H_k^\nu\right|^2 = \sum_{\nu=1}^{N} \gamma_k^\nu, \quad k = 0, 1, \ldots, K-1 \tag{28}$$

where $\gamma_k^\nu \triangleq \frac{\rho}{p\rho+(1-p)} \left|H_k^\nu\right|^2$ denotes the instantaneous SINR for the kth subchannel of the νth channel at the output of MRC. We assume the independence between different diversity reception branches, then H_k^ν is independent of H_k^j if $j \neq \nu$, and therefore γ_k^ν is independent of γ_k^j if $j \neq \nu$.

3.2 SER of the MRC-OFDM receiver with pulse blanking over Rayleigh fading channel

For the Rayleigh fading channel, the frequency response of the kth subchannel of the νth receive branch $H_k^\nu = \sum_{l=0}^{L_\nu - 1} h_l^\nu e^{-j2\pi \frac{kl}{K}}$ is a complex Gaussian RV of mean zeros and variance one, thus $\left|H_k^\nu\right|^2$ is χ^2 distributed with 2 degrees of freedom and $E\left\{\left|H_k^\nu\right|^2\right\} = 1$.

Considering $\rho / (p\rho + (1-p))$ is a constant when the probability of impulsive noise occurrence p is given, γ_k^ν is also χ^2 distributed with 2 degrees of freedom and mean $\bar{\gamma} = \rho / (p\rho + (1-p))$. Therefore, the probability density function (PDF) of γ_k^ν is given by [20]

$$p\left(\gamma_k^\nu\right) = \frac{1}{\bar{\gamma}} e^{\frac{-\gamma_k^\nu}{\bar{\gamma}}}, \gamma_k^\nu \geq 0, k = 0, 1, \ldots, K-1, \nu = 1, 2, \ldots, N \tag{29}$$

The moment generating function (MGF) of γ_k^ν can be obtained by applying the Laplace transform to $p\left(\gamma_k^\nu\right)$ with the exponent reversed in sign and is given by [21]

$$M_{\gamma_k^\nu}(s) = \frac{1}{1 - s\bar{\gamma}}, k = 0, 1, \ldots, K-1, \nu = 1, 2, \ldots, N \tag{30}$$

Note that the MGF of the sum of independent RVs is the product of the MGFs of individual RVs [21]. Using Eqs. (28) and (30), the MGF of the combined SINR with MRC of the kth subchannel γ_k becomes

$$M_{\gamma_k}(s) = \prod_{\nu=1}^{N} M_{\gamma_k^\nu}(s) = \frac{1}{(1 - s\bar{\gamma})^N}, \quad k = 0, \ldots, K-1 \tag{31}$$

Using the result in [21], the SER of the kth subchannel for the OFDM receiver with M-phase-shift keying (PSK) modulation over Rayleigh fading channel can be expressed as

$$\text{SER}_{\text{MPSK},k}^{\text{Rayleigh}} = \frac{1}{\pi} \int_0^{(M-1)\pi/M} M_{\gamma_k}\left(\frac{-g_{\text{psk}}}{\sin^2\theta}\right) \text{d}\theta \tag{32}$$

where $g_{\text{psk}} = \sin^2(\pi/M)$. For large $\bar{\gamma}$, the average SER of Eq. (32) behaves as [16]

$$\text{SER}_{\text{MPSK},k}^{\text{Rayleigh}} \simeq \frac{C_{\text{PSK}}(N, M)}{\bar{\gamma}^N} \tag{33}$$

where

$$C_{\text{PSK}}(N, M) = \frac{1}{[2\sin(\pi/M)]^{2N}} \left[\binom{2N}{N} \frac{M-1}{M} - \sum_{j=1}^{N} \binom{2N}{N-j} (-1)^j \frac{\sin(2\pi j/M)}{\pi j} \right] \tag{34}$$

The SER of the kth subchannel for the OFDM receiver with M-quadrature amplitude modulation (QAM) over Rayleigh fading channel can be expressed as

$$\text{SER}_{\text{MQAM},k}^{\text{Rayleigh}} = \frac{4}{\pi}\left(1 - \frac{1}{\sqrt{M}}\right) \int_0^{\pi/2} M_{\gamma_k}\left(-\frac{g_{\text{QAM}}}{\sin^2\theta}\right) \text{d}\theta - \frac{4}{\pi}\left(1 - \frac{1}{\sqrt{M}}\right)^2 \int_0^{\pi/4} M_{\gamma_k}\left(-\frac{g_{\text{QAM}}}{\sin^2\theta}\right) \text{d}\theta \tag{35}$$

where $g_{\text{QAM}} = 3/(2(M-1))$. For large $\bar{\gamma}$, the average SER of Eq. (35) behaves as

$$\text{SER}_{\text{MQAM},k}^{\text{Rayleigh}} \simeq \frac{C_{\text{QAM}}(N, M)}{\bar{\gamma}^N} \tag{36}$$

where

$$C_{\text{QAM}}(N, M) = \frac{1}{2^{2N}} \left(\frac{\sqrt{M}-1}{\sqrt{M}}\right)^2 {g_{\text{QAM}}}^{-N} \times \left[\binom{2N}{N} \left(\frac{2\sqrt{M}}{\sqrt{M}-1} - 1\right) - \frac{4}{\pi} \sum_{j=1}^{N} \binom{2N}{N-j} \frac{(-1)^{(j+1)/2}}{j} \right] \tag{37}$$

In the SER expressions given in Eqs. (32), (33), (35), and (36), the SER of the kth subchannel is independent of the subchannel index, which indicates that pulse blanking has the same effect on the error performance of each subchannel of the MRC-OFDM receiver.

In particular, for the binary PSK (BPSK) modulation, the closed-form expression for the integral in Eq. (32) becomes [16]

$$\mathrm{SER}_{\mathrm{BPSK},k}^{\mathrm{Rayleigh}} = \left[\frac{1}{2}(1-\mu)\right]^N \sum_{j=0}^{N-1} \binom{N-1+j}{j} \times \left[\frac{1}{2}(1+\mu)\right]^j \tag{38}$$

where $\mu = \sqrt{\bar{\gamma}/(1+\bar{\gamma})}$.

The exact expression in Eq. (38) provides insight into a few special cases. (i) When there is no interference, i.e., $p = 0$, $\bar{\gamma} = \rho$, Eq. (38) reduces to the symbol error probability of a conventional Nth-order space diversity receiver employing MRC. (ii) When there is interference, i.e., $p \neq 0$, and in the limiting case the input SNR is large, i.e., $\rho \to \infty$, $\lim_{\rho\to\infty} \bar{\gamma} = 1/p$, thus, there will be an error floor for the SER performance curve. Considering a small p value (less than 0.1) fulfilling the condition $\bar{\gamma} \gg 1$, the approximate theoretical expression of the error floor behaves as $\left(\frac{p}{4}\right)^N \binom{2N-1}{N}$. Therefore, the error floor decreases proportionally with the Nth power of the probability of impulsive noise occurrence p at an Nth-order space diversity. For a given p value, the error floor can be efficiently reduced as the number of receive antenna increases. The same conclusion can be reached based on the approximate expressions in Eqs. (33) and (36).

3.3 SER of the MRC-OFDM receiver with pulse blanking over Ricean fading channel

For the Ricean fading channel, h_0^ν is assumed to be a nonzero mean complex Gaussian RV, i.e., $h_0^\nu \sim \mathcal{CN}\left(u_\nu, \delta_0^{\nu 2}\right)$, $\left\{h_l^\nu, l = 1, \ldots, L_\nu - 1\right\}$ are assumed to be complex Gaussian RVs, i.e., $h_l^\nu \sim \mathcal{CN}\left(0, \delta_l^{\nu 2}\right)$. The channel power is normalized to 1, i.e., $|u_\nu|^2 + \sum_{l=0}^{L-1} \left|\delta_l^\nu\right|^2 = 1$, and the Ricean factor of the νth channel is defined as $K_\nu \triangleq |u^\nu|^2 \Big/ \sum_{l=0}^{L-1} \left|\delta_l^\nu\right|^2$. Hence, the frequency response of the kth subchannel H_k^ν is distributed according to complex Gaussian with mean u^ν and variance $\sum_{l=0}^{L-1} \left|\delta_l^\nu\right|^2 - |u^\nu|^2$. Furthermore, $\left|H_k^\nu\right|^2$ is noncentral χ^2 distributed with 2 degrees of freedom and $E\left\{|H_k^\nu|^2\right\} = 1$.

Considering $\rho/(p\rho + (1-p))$ is a constant when the probability of impulsive noise occurrence p is given, γ_k^ν is also according to noncentral χ^2 distributed with 2 degrees of freedom with mean $\bar{\gamma} = \rho/(p\rho + (1-p))$. Therefore, the PDF of γ_k^ν is given by [15]

$$p\left(\gamma_k^\nu\right) = \frac{(1+K_\nu)\, e^{-\frac{(1+K^\nu)\gamma_k^\nu}{\bar{\gamma}}}}{\bar{\gamma}} I_0\left(2\sqrt{\frac{K_\nu(1+K_\nu)\gamma_k^\nu}{\bar{\gamma}}}\right) \tag{39}$$

where $I_0(\cdot)$ is the zero-order modified Bessel function of the first kind. The MGF of γ_k^ν can be expressed as

$$M_{\gamma_k^\nu}(s) = \frac{1+K_\nu}{1+K_\nu - s\bar{\gamma}} \exp\left(\frac{K_\nu s\bar{\gamma}}{1+K_\nu - s\bar{\gamma}}\right) \tag{40}$$

Then, the MGF of the combined SINR can be written as

$$\begin{aligned} M_{\gamma_k}(s) &= \prod_{\nu=1}^{N} M_{\gamma_k^\nu}(s) \\ &= \prod_{\nu=1}^{N} \left\{\frac{1+K_\nu}{1+K_\nu - s\bar{\gamma}} \exp\left(\frac{K_\nu s\bar{\gamma}}{1+K_\nu - s\bar{\gamma}}\right)\right\} \end{aligned} \tag{41}$$

Using the result in [21], the SER of the kth subchannel for the OFDM receiver with M-PSK modulation over Ricean fading channel can be expressed as

$$\mathrm{SER}_{\mathrm{MPSK},k}^{\mathrm{Ricean}} = \frac{1}{\pi}\int_0^{(M-1)\pi/M} M_{\gamma_k}\left(-\frac{g_{\mathrm{psk}}}{\sin^2\theta}\right)\mathrm{d}\theta \tag{42}$$

For large $\bar{\gamma}$, the average SER of Eq. (42) behaves as

$$\mathrm{SER}_{\mathrm{MPSK},k}^{\mathrm{Ricean}} \simeq \frac{\exp\left(-\sum_{\nu=1}^{N} K_\nu\right) C_{\mathrm{PSK}}(N,M)}{\bar{\gamma}^N} \times \prod_{\nu=1}^{N}(1+K_\nu) \tag{43}$$

The SER of the kth subchannel for the OFDM receiver with M-QAM modulation over Ricean fading channel can be expressed as

$$\begin{aligned} \mathrm{SER}_{\mathrm{MQAM},k}^{\mathrm{Ricean}} = {} & \frac{4\left(\sqrt{M}-1\right)}{\pi\sqrt{M}} \int_0^{\pi/2} M_{\gamma_k}\left(-\frac{g_{\mathrm{QAM}}}{\sin^2\theta}\right)\mathrm{d}\theta \\ & - \frac{4\left(\sqrt{M}-1\right)^2}{\pi M} \int_0^{\pi/4} M_{\gamma_k}\left(-\frac{g_{\mathrm{QAM}}}{\sin^2\theta}\right)\mathrm{d}\theta \end{aligned} \tag{44}$$

For large $\bar{\gamma}$, the average SER of Eq. (44) behaves as [21]

$$\mathrm{SER}_{\mathrm{MQAM},k}^{\mathrm{Ricean}} \simeq \frac{\exp\left(-\sum_{\nu=1}^{N} K_\nu\right) C_{\mathrm{QAM}}(N,M)}{\bar{\gamma}^N} \times \prod_{\nu=1}^{N}(1+K_\nu) \tag{45}$$

Also, the SER derived above is only for the kth subcarrier. It has to be averaged over all the subcarriers.

Table 1 System and channel parameters

Parameters	Value
System parameters	
Modulator	BPSK, 8PSK, 16QAM
Subcarrier number	512
Data subcarrier number	512
Cyclic prefix	16
Channel parameters	
Channel models	Rayleigh (10 paths)
	Ricean (10 paths, $\{K_v\} = 10$ dB)
Impulsive noise model	Bernoulli-Gaussian
Probability of interference occurrence	p (see figures)
Receiver parameters	
Number of receive antenna	$N = 2, 4$
Channel estimation	Ideal channel estimation
Channel equalization	ZF equalization

Comparing Eq. (44) with Eq. (33), Eq. (45), and Eq. (36), we find that for the specific Ricean factors, the same conclusion presented in Section 3.2 can be reached based on the approximate expressions in Eqs. (45) and (46).

4 Numerical results

4.1 System and channel parameters

The system and channel parameters are listed in Table 1.

4.2 Symbol error performance curves

To verify the accuracy of the theoretical formulas derived in the previous sections, we compare the SER performances of the theoretical formulas with the results of computer simulations for Rayleigh and Ricean fading channels. Figures 3, 4, 5, 6, 7, 8, 9, and 10 show the theoretical and simulated SER versus SNR ($10\log_{10}(\rho)$) performance curves of the MRC-OFDM receiver with pulse blanking.

Figures 3 and 4 show the SER performances of the MRC-OFDM receiver with pulse blanking for BPSK modulation over Rayleigh fading channel for $N = 2$ and $N = 4$ receive antennas. Each figure contains four pairs of curves, which shows the theoretical and simulated SER of the OFDM receiver with pulse blanking at different p values. In both figures, it can be seen that theoretical results correspond well with the simulation results.

From Fig. 3, the theoretical and simulated error floor versus the probability of impulsive noise occurrence p are listed in Table 2. From the table, the simulated observations of the error floor achieve a good agreement with the theoretical calculations. We see that the error floor decreases as the probability of impulsive noise occurrence decreases. Further, the error floor decreases proportionally with the Nth power of the probability of impulsive noise occurrence p. Comparing the two figures, it is shown that the error floor is efficiently reduced for $N = 4$ receive antennas compared with $N = 2$ for the same p value.

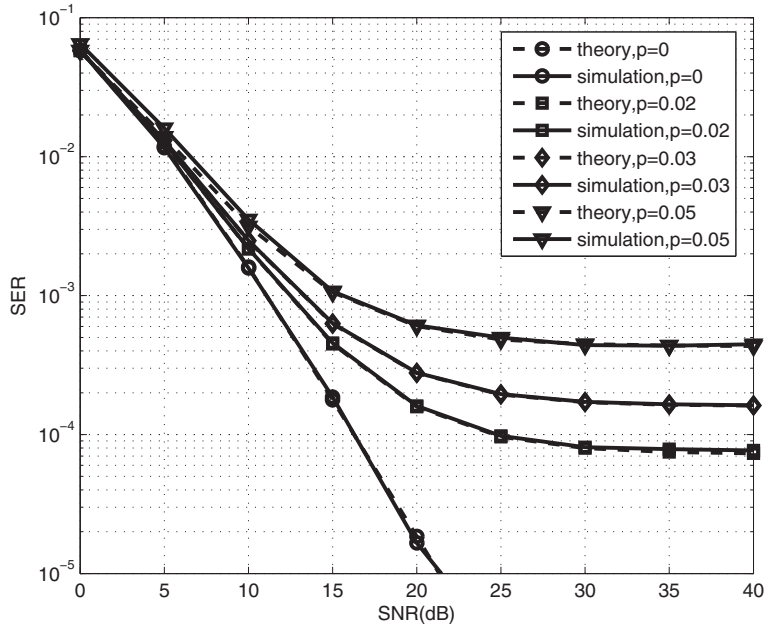

Fig. 3 SER performances of the MRC-OFDM receiver with pulse blanking for BPSK modulation over Rayleigh fading channel for $N = 2$ receive antennas

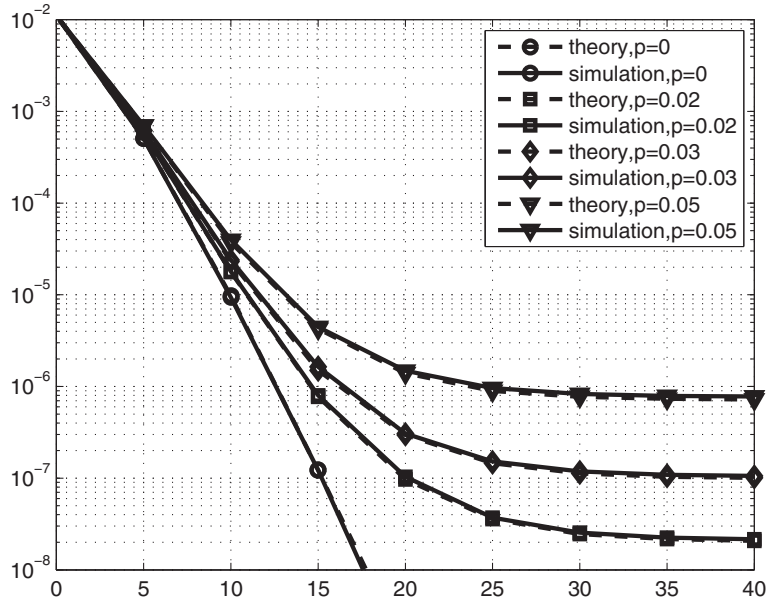

Fig. 4 SER performances of the MRC-OFDM receiver with pulse blanking in case of BPSK modulation over Rayleigh fading channel for $N = 4$ receive antennas

Similarly, for the same receiver and channel, Figs. 5 and 6 show the SER performances for 16QAM modulation with $N = 2$ and $N = 4$ receive antennas, respectively. From the four pairs of curves in each figure, the theoretical results correspond well with the simulation results and derive the same analysis as that in Figs. 3 and 4.

Figures 7 and 8 show the SER performances of the MRC-OFDM receiver with pulse blanking for 8PSK modulation over Ricean fading channel with Ricean factors $\{K_\nu\} = 10$ dB for $N = 2$ and $N = 4$ receive antennas, respectively. Similar to the previous paragraph, from the four pairs of curves in each figure, the theoretical results agree

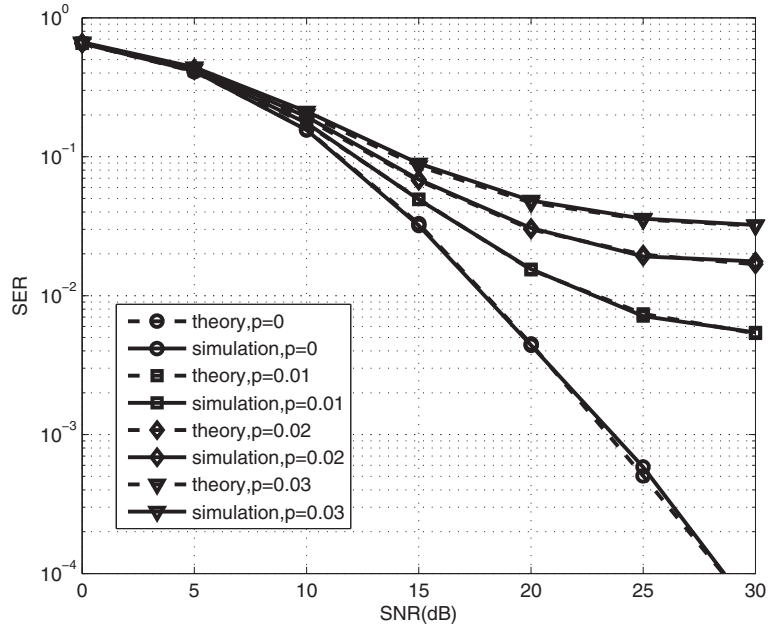

Fig. 5 SER performances of the MRC-OFDM receiver with pulse blanking for 16QAM modulation over Rayleigh fading channel for $N = 2$ receive antennas

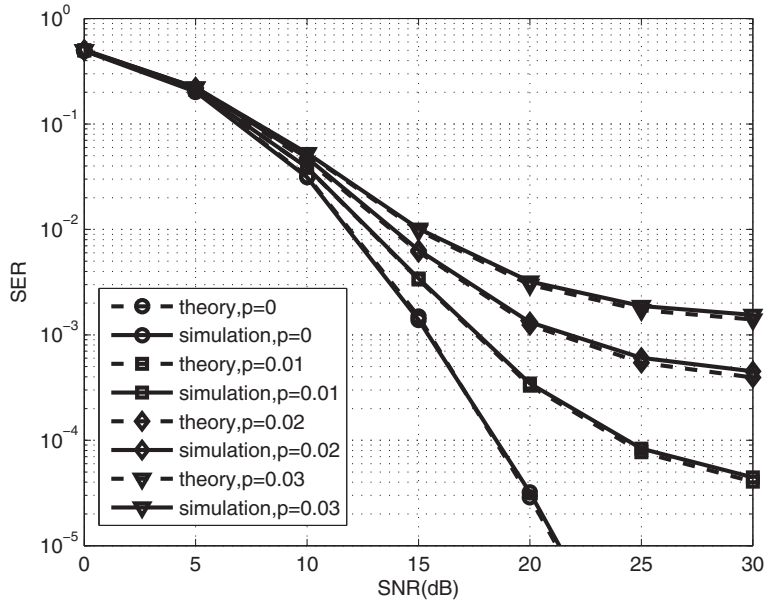

Fig. 6 SER performances of the MRC-OFDM receiver with pulse blanking for 16QAM modulation over Rayleigh fading channel for $N = 4$ receive antennas

well with the simulation results. We arrive then with the same analysis as for Figs. 3 and 4.

Similarly, for the same receiver and channel, Figs. 9 and 10 show the SER performances for 16QAM modulation with $N = 2$ and $N = 4$ receive antennas, respectively. Again, from the four pairs of curves of in each figure, the theoretical results correspond well with the simulation results and yield the same analysis as for Figs. 3 and 4.

5 Conclusions

In this paper, we studied the symbol error performance of the MRC-OFDM receiver with pulse blanking over frequency selective fading channel. The closed-form expression of the SINR for the MRC-OFDM receiver with pulse blanking is derived. The SER of the MRC-OFDM receiver with pulse blanking over both Rayleigh and Ricean fading channels are also given. The simulation results validate

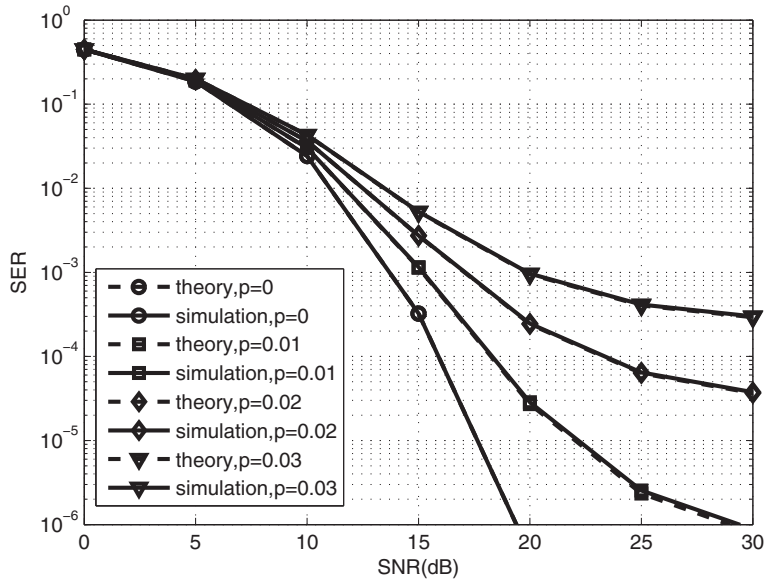

Fig. 7 SER performances of the MRC-OFDM receiver with pulse blanking in case of 8PSK modulation over Ricean fading channel for $N = 2$ receive antennas

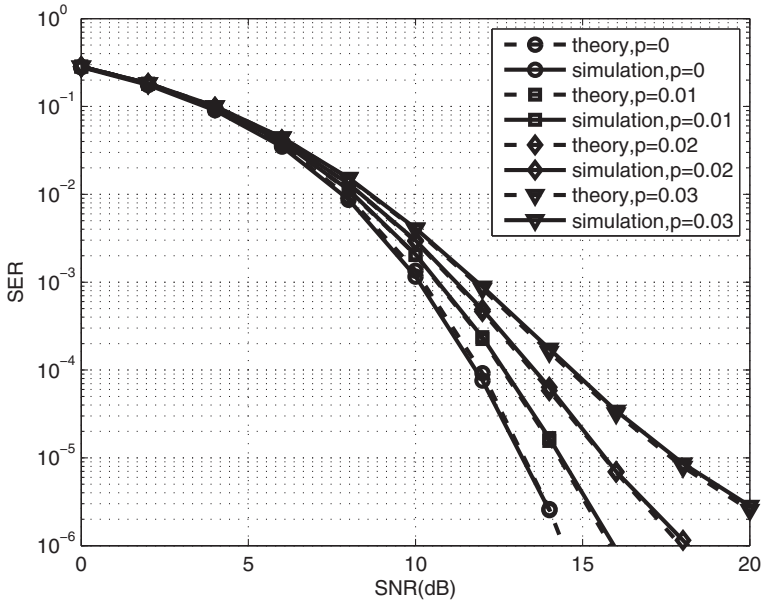

Fig. 8 SER performances of the MRC-OFDM receiver with pulse blanking in case of 8PSK modulation over Ricean fading channel for $N = 4$ receive antennas

the correctness of our derived formulas. The following conclusions are obtained: (i) the pulse blanking has same effect on the error performance of each subchannel of the MRC-OFDM receiver; (ii) the error floor for the SER performance is observed for the MRC-OFDM receiver with pulse blanking and the error floor depends on the probability of impulsive noise occurrence and the number of receive antenna; and (ii) the developed analysis method in this paper can be extended to the case of the Middleton class A noise environment and the error floor for the SER performance is determined by the probability of the Middleton class A impulsive noise occurrence.

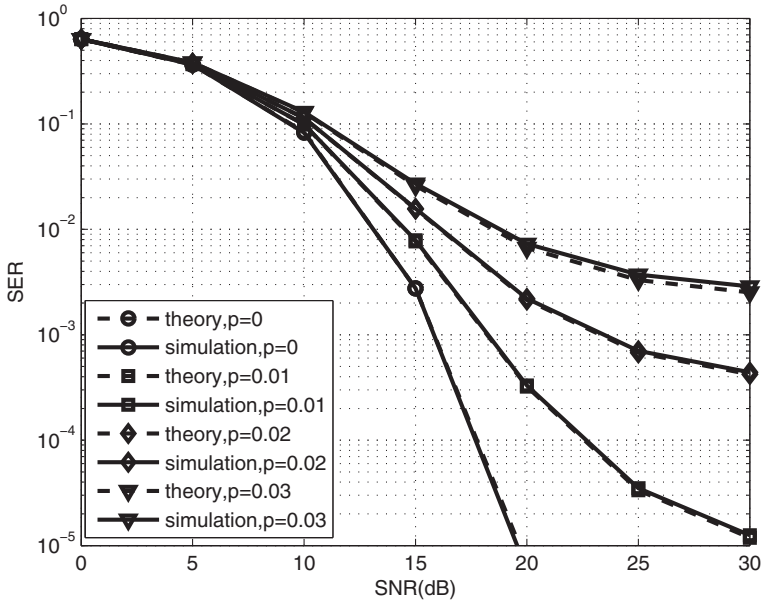

Fig. 9 SER performances of the MRC-OFDM receiver with pulse blanking for 16QAM modulation over Ricean fading channel with $N = 2$ receive antennas

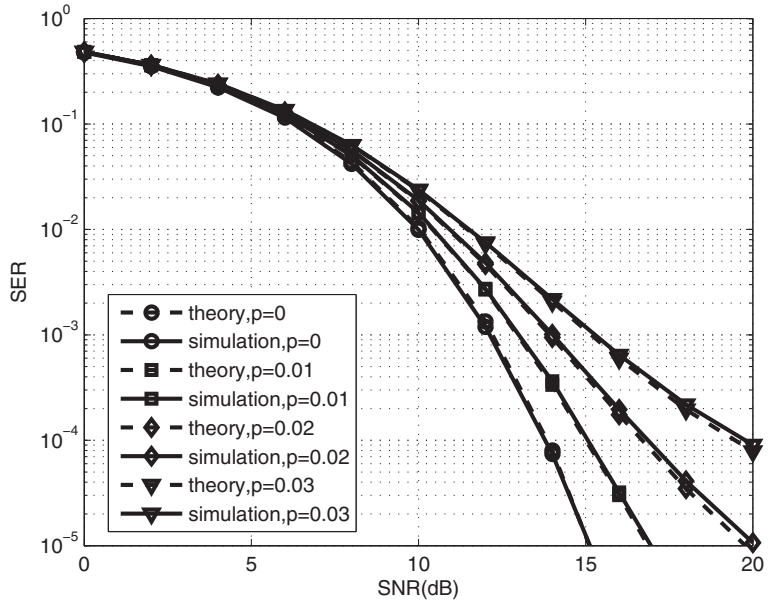

Fig. 10 SER performances of the MRC-OFDM receiver with pulse blanking for 16QAM modulation over Ricean fading channel with $N = 4$ receive antennas

Appendix

From Eq. (24), the variance of interference noise term can be calculated as

$$V_{\mathrm{ar}}(W_k) = E\left\{|W_k|^2\right\} - \left(E\left\{|W_k|\right\}\right)^2 \tag{46}$$

Considering that H_k^{ν} and $H_k^{j}\left(j \neq \nu\right)$ are statistically independent, the first term of Eq. (46) is obtained as

$$E\left\{|W_k|^2\right\} = \frac{1}{K}\sum_{\nu=1}^{N}\left|H_k^{\nu}\right|^2 \sum_{n=0}^{K-1}\left(E\left\{\left|\tilde{i}_n^{\nu}\right|^2\right\} + E\left\{\left|\tilde{n}_n^{\nu}\right|^2\right\}\right) \tag{47}$$

By using Eq. (17) and considering b_n^{ν} , s_m and h_l^{ν} are statistically independent, $E\left\{\left|\tilde{i}_n^{\nu}\right|^2\right\}$ can be calculated as

$$\begin{aligned} E\left\{\left|\tilde{i}_n^{\nu}\right|^2\right\} &= E\left\{\left|-b_n^{\nu}\sum_{m=0}^{K-1} s_m h_{(n-m) \bmod K}^{\nu}\right|^2\right\} \\ &= E\left\{\left|b_n^{\nu}\right|^2\right\} E\left\{|s_m|^2\right\} \sum_{m=0}^{K-1} E\left\{\left|h_{(n-m) \bmod K}^{\nu}\right|^2\right\} \\ &= p\sigma_S^2 \end{aligned} \tag{48}$$

Table 2 Impact of probability of impulsive noise occurrence on the error floor

p	Error floor (theory)	Error floor (simulation)
0.02	7.50e−005	7.0e−005
0.03	1.69e−004	1.5e−004
0.05	4.69e−004	4.5e−004

By using Eq. (18) and considering that b_n^{ν} is independent of n_n^{ν} , $E\left\{|\tilde{n}_n|^2\right\}$ can be calculated as

$$\begin{aligned} E\left\{|\tilde{n}_n|^2\right\} &= E\left\{\left|\left(1-b_n^{\nu}\right)n_n\right|^2\right\} \\ &= (1-p)\,\delta_n^2 \end{aligned} \tag{49}$$

By using Eqs. (17) and (18) and keeping $E\{s_m\} = 0$ and $E\{n_n\} = 0$ in mind, it is easy to find $E\left\{\tilde{i}_n\right\} = 0$ and $E\{\tilde{n}_n\} = 0$. Furthermore, the second term of (46) can be calculated as $\left(E\{|W_k|\}\right)^2 = 0$. Finally, the variance of the interference noise term W_k can be obtained as

$$V_{\mathrm{ar}}(W_k) = \left[p\sigma_S^2 + (1-p)\,\delta_n^2\right]\sum_{\nu=1}^{N}\left|H_k^{\nu}\right|^2 \tag{50}$$

Competing interests
The authors declare that they have no competing interests.

Acknowledgements
This work was supported in part by National Natural Science Foundation of China under Grants No. U1233117 and No. 61271404.

Author details
[1]Tianjin Key Lab for Advanced Signal Processing, Civil Aviation University of China, 30030 Tianjin, China. [2]Communication Research Center, Harbin Institute of Technology, 150080 Harbin, China. [3]College of Electronic and Information Engineering, BeiHang University, 100191 Beijing, China.

Received: 14 September 2015 Accepted: 17 April 2016
Published online: 18 May 2016

References

1. N Neji, R de Lacerda, A Azoulay, T Letertre, O Outtier, Survey on the future aeronautical communication system and its development for continental communications. Veh. Technol. IEEE Trans. **62**(1), 182–191 (2013)

2. M Ghosh, Analysis of the effect of impulse noise on multicarrier and single carrier QAM systems. Commun. IEEE Trans. **44**(2), 145–147 (1996)
3. YH Ma, PL So, E Gunawan, Performance analysis of OFDM systems for broadband power line communications under impulsive noise and multipath effects. Power Delivery IEEE Trans. **20**(2), 674–682 (2005)
4. P Lewis, A Tutorial on Impulsive Noise in COFDM Systems (2001). http://www.dtg.org.uk. Accessed May 2001
5. NP Cowley, A Payne, M Dawkins, COFDM tuner with impulse noise reduction. EP1180851 (2003). http://www.freepatentsonline.com/EP1180851B1.html
6. CR Nokes, OP Haffenden, JD Mitchell, AP Robinson, JH Stott, A Wiewiorka, Detection and removal of clipping in multicarrier receivers. **EP1043874** (2000). http://www.freepatentsonline.com/EP1043874A2.html
7. SV Zhidkov, Performance analysis and optimization of OFDM receiver with blanking nonlinearity in impulsive noise environment. Veh. Technol. IEEE Trans. **55**(1), 234–242 (2006)
8. U Epple, M Schnell, in *Global Communications Conference (GLOBECOM), 2012*. Adaptive threshold optimization for a blanking nonlinearity in OFDM receivers (IEEE, Anaheim CA, USA, 2012), pp. 3661–3666
9. S Brandes, U Epple, M Schnell, in *Global Telecommunications Conference, 2009. GLOBECOM 2009*. Compensation of the impact of interference mitigation by pulse blanking in OFDM systems (IEEE, Honolulu HI, USA, 2009), pp. 1–6
10. C-H Yih, Iterative interference cancellation for OFDM signals with blanking nonlinearity in impulsive noise channels. Signal Process. Lett. IEEE. **19**(3), 147–150 (2012)
11. D Darsena, G Gelli, F Melito, F Verde, ICI-free equalization in OFDM systems with blanking preprocessing at the receiver for impulsive noise mitigation. Signal Process. Lett. IEEE. **22**(9), 1321–1325 (2015)
12. C Tepedelenlioglu, P Gao, in *Global Telecommunications Conference, 2004. GLOBECOM '04*. On diversity reception over fading channels with impulsive noise (IEEE, Washington, DC, USA, 2004), pp. 3676–3680
13. P Gao, C Tepedelenlioglu, Space-time coding over fading channels with impulsive noise. Wireless Commun. IEEE Trans. **6**(1), 220–229 (2007)
14. R Savoia, F Verde, Performance analysis of distributed space-time block coding schemes in middleton class-a noise. Veh. Technol. IEEE Trans. **62**(6), 2579–2595 (2013)
15. J Lee, C Tepedelenlioglu, Space-time coding over fading channels with stable noise. Veh. Technol. IEEE Trans. **60**(7), 3169–3177 (2011)
16. A Nasri, R Schober, IF Blake, Performance and optimization of amplify-and-forward cooperative diversity systems in generic noise and interference. Wireless Commun. IEEE Trans. **10**(4), 1132–1143 (2011)
17. U Epple, K Shibli, M Schnell, in *Communications (ICC), 2011 IEEE International Conference On*. Investigation of blanking nonlinearity in OFDM systems (IEEE, Kyoto, Japan, 2011), pp. 1–5
18. HT Liu, ZS Yin, XJ Zhang, Performance analysis of OFDM receiver with pulse blanking in frequency selective Rayleigh fading channel. J. Beijing University Posts Telecommun. **38**(4), 29–32 (2015)
19. Y Li, G Stuber, *Orthogonal Frequency Division Multiplexing for Wireless Communications*. (Springer, New York, 2006)
20. JG Proakis, *Digital Communications Fourth Edition*, 4nd edn. (Publishing House of Electronics Industry, Beijing, 2011)
21. M-S Simon, MK Alouini, *Digital Communications over Fading Channels 2nd Edition*, 2nd edn. (Wiley, New York, 2005)